M. Ernzerhof, K. Burke, and J. P. Perdew, in *Recent Developments in Density Functional Theory, Theoretical and Computational Chemistry*, edited by J. M. Seminario (Elsevier, Amsterdam, 1997).

Density functional theory, the exchange hole, and the molecular bond

Matthias Ernzerhof [a], Kieron Burke [b], and John P. Perdew [a]

[a]Department of Physics and Quantum Theory Group,
Tulane University, New Orleans, LA 70118

[b] Department of Chemistry,
Rutgers University, Camden, NJ 08102

The Perdew-Wang 91 (PW91) generalized gradient approximation (GGA) derives from a model for the exchange-correlation hole. The basic concepts of the exchange-correlation hole are explained, and the relation to wavefunction methods such as Hartree-Fock is emphasized. To verify the construction of the PW91 functional, we compare the PW91 model for the exchange hole with the exact exchange hole. We study the change of the exchange hole upon atomization of the hydrogen molecule, and find that the PW91 model gives an accurate description of this change. For multiply-bonded molecules like N_2, PW91 provides too much exchange interaction between electrons in neighboring bonds. The largest PW91 errors occur not in the atom but in the molecule; we discuss how errors in the exchange and correlation energies tend to cancel. The fundamentals of the coupling-constant integration are explained, and the coupling-constant dependence of the atomization energy is investigated. Finally, we discuss hybrids which admix a fraction of the exact exchange energy with density functional approximations.

1. Introduction

Density functional theory [1–3] has become a valuable tool for chemistry, one which complements and augments the traditional quantum chemical methods which implicitly or explicitly construct interacting wavefunctions. The workhorse of the wavefunction methods is the Hartree-Fock (HF) approximation. The inherent limitations of Hartree-Fock have been studied over the years, and much is known about the reliability of this and other wavefunction methods when applied to specific systems [4]. Furthermore, the theory of the HF method is also well understood, and the performance of this and other wavefunction methods can be predicted from an understanding of the basic elements of the theory [4].

Density functional methods have become popular in chemistry only recently, so the formal framework of this theory and consequences for the performance of the approximate density functionals are less well understood. In the present article we therefore discuss the basic elements of density functional theory, and illustrate the formalism with calculations on small representative systems.

Kohn and Sham [3] showed that the exact ground-state energy E and spin-densities $\rho_\sigma(\mathbf{r})$ for N electrons in the presence of an external potential $v(\mathbf{r})$ can be found in principle

by solving a selfconsistent one-electron Schrödinger equation:

$$\left[-\frac{1}{2}\nabla^2 + v^\sigma_{eff}(\mathbf{r})\right]\phi_i(\mathbf{r},\sigma) = \epsilon_i\ \phi_i(\mathbf{r},\sigma), \tag{1}$$

$$\rho_\sigma(\mathbf{r}) = \sum_i^{occ} |\phi_i(\mathbf{r},\sigma)|^2, \tag{2}$$

where the sum runs over all occupied Kohn-Sham orbitals ϕ_i and $\sigma =\uparrow$ or $\downarrow$. Thus Kohn-Sham density functional theory resembles Hartree-Fock theory, with two changes: the Hartree-Fock exchange energy E_x^{HF} is replaced by the density functional $E_{xc}[\rho_\uparrow,\rho_\downarrow]$ for the exchange-correlation energy, and the nonlocal Hartree-Fock exchange potential $v_x^\sigma(\mathbf{r},\mathbf{r}')$ is replaced by the local exchange correlation potential $v_{xc}^\sigma(\mathbf{r})$ as a component of the selfconsistent effective potential $v^\sigma_{eff}(\mathbf{r})$. This local potential $v_{xc}^\sigma(\mathbf{r})$ is the functional derivative $\delta E_{xc}/\delta\rho_\sigma(\mathbf{r})$, and so depends upon $\rho_\uparrow$ and $\rho_\downarrow$.

Typically 50% or more of the energy needed to atomize a molecule is exchange-correlation energy. Because the exact density functional $E_{xc}[\rho_\uparrow,\rho_\downarrow]$ is unknown, it must be approximated. The local spin density approximation (LSD) [3]

$$E_{xc}^{LSD}[\rho_\uparrow,\rho_\downarrow] = \int d^3r\ \rho(\mathbf{r})\epsilon_{xc}(\rho_\uparrow(\mathbf{r}),\rho_\downarrow(\mathbf{r})), \tag{3}$$

where $\rho = \rho_\uparrow + \rho_\downarrow$, utilizes the exchange-correlation energy per electron of a uniform electron gas, $\epsilon_{xc}(\rho_\uparrow,\rho_\downarrow)$, which is accurately known [5]. (In the uniform-gas or jellium model, the electron density is neutralized by a rigid infinite uniform background of positive charge.) Clearly this approximation is valid in the limit of spin densities $\rho_\sigma(\mathbf{r})$ that vary slowly over space. LSD has a long and mostly triumphant history in solid state physics, where it routinely predicts correct crystal structures, lattice constants, bulk moduli, and vibrational frequencies. But LSD has been much less popular in quantum chemistry, where it seriously overestimates the atomization energies of molecules.

The first systematic correction to LSD is the second-order gradient expansion approximation (GEA) [6,7]:

$$E_{xc}^{GEA}[\rho_\uparrow,\rho_\downarrow] = E_{xc}^{LSD}[\rho_\uparrow,\rho_\downarrow] + \sum_{\sigma,\sigma'}\int d^3r\ C_{xc}^{\sigma,\sigma'}(\rho_\uparrow,\rho_\downarrow)\nabla\rho_\sigma\cdot\nabla\rho_{\sigma'}/\rho_\sigma^{2/3}\rho_{\sigma'}^{2/3}. \tag{4}$$

But, for real atoms, molecules, and solids, GEA is *less* accurate [6] than LSD. This fact shows that the electron densities of real systems are *not* close to the slowly-varying limit. The true reasons for the success of LSD in solid state calculations were identified by Gunnarsson and Lundqvist [8], who showed that LSD preserves certain properties of the exact exchange-correlation hole which constrain the energy to a reasonable value. Later Langreth and Perdew [9] showed that GEA does *not* preserve these properties.

The GEA form of Eq. 4 is semi-local, as is the generalized gradient approximation (GGA)

$$E_{xc}^{GGA}[\rho_\uparrow,\rho_\downarrow] = \int d^3r\ \rho\ \epsilon_{xc}(\rho_\uparrow,\rho_\downarrow,\nabla\rho_\uparrow,\nabla\rho_\downarrow), \tag{5}$$

which approximately sums up an infinite series in powers of $\nabla\rho_\sigma$. It is the success of the GGA's that has attracted the current intense interest in density functionals within

the quantum chemistry community. Some GGA's have been constructed semi-empirically [6,10–15], with parameters fitted to experiment, while others have been constructed *ab initio* [16–19], by starting from the gradient expansion and then restoring those properties of the exchange-correlation hole that are responsible for the success of the LSD in solids.

All of the *ab initio* GGA's, and some but not all of the semi-empirical ones, are "locally-based" or exact for the uniform electron gas, i.e.,

$$\epsilon_{xc}(\rho_\uparrow, \rho_\downarrow, \nabla\rho_\uparrow = 0, \nabla\rho_\downarrow = 0) = \epsilon_{xc}(\rho_\uparrow, \rho_\downarrow). \tag{6}$$

Eq. 6 is a powerful constraint which keeps a locally-based GGA from going astray, a constraint that is particularly (but not only) relevant to solid state applications.

While the Hartree-Fock approximation underbinds atoms in molecules, and LSD overbinds them, GGA's achieve a useful accuracy [18,20–22]. This accuracy can be further boosted by constructing hybrids [14,23–28] that mix GGA with a fraction of the exact or Hartree-Fock exchange. While these methods do not compete in accuracy with Configuration Interaction and Coupled-Cluster techniques [29] applied to small systems, they do bring medium- and large-size molecules within the reach of quantitative theory.

Among the gradient-corrected density functionals, the generalized gradient approximation of Perdew, Wang, and Burke [16–19] offers the possibility for a detailed analysis, since it is based on a model for the exchange-correlation hole (or equivalently a model for the pair density). This makes it possible to compare exchange-correlation holes predicted by the GGA approximation with exchange-correlation holes obtained from accurate wavefunction calculations for small systems.

In density functional theory, as opposed to wavefunction theory, there are few practical reasons to distinguish the exchange limit, and in fact there are many arguments not to do so. The exchange limit is usually not well approximated by local and semi-local density functionals, in contrast to the full interacting case. Somewhat paradoxically, density functional approximations to the exchange limit are often a good approximation to experimental results, while an exact description of exchange is not. In particular, atomization energies calculated within the local density approximation for exchange are in fair agreement with experimental results [26]. The conventional wisdom is that we have little reason to put much effort into the construction of functionals which reproduce the exact exchange energy; it is more promising to improve functionals for exchange and correlation together. On the other hand, progress in density functional theory is achieved by analyzing density functionals to understand how they work and to isolate features of functionals which can be further improved. In this sense, it is of theoretical interest to analyze the exchange limit of density functionals. In this work we therefore focus first on exchange. We hope that this approach will make the article more accessible to the reader familiar with traditional quantum chemistry methods, in which the Hartree-Fock approximation often serves as a well-defined starting point.

The Hartree-Fock exchange energy is

$$E_x = -\frac{1}{2}\sum_\sigma \int d^3r \int d^3r' |\sum_i^{occ} \phi_i^*(\mathbf{r},\sigma)\phi_i(\mathbf{r}',\sigma)|^2/|\mathbf{r}'-\mathbf{r}|, \tag{7}$$

where the ϕ_i are Hartree-Fock orbitals, while the exact exchange energy of Kohn-Sham theory is given by the same expression evaluated using Kohn-Sham orbitals. Clearly the

exchange energy is the sum of two contributions, one from the spin-up electrons and the other from spin-down. It contains a self-interaction correction to the Hartree approximation, plus a further reduction of the Coulomb energy V_{ee} due to the Pauli principle, which keeps parallel-spin electrons apart. The exact Kohn-Sham density functional for exchange has two very simple scaling properties:

$$E_x[\rho_\uparrow, \rho_\downarrow] = \frac{1}{2}E_x[2\rho_\uparrow] + \frac{1}{2}E_x[2\rho_\downarrow] \tag{8}$$

where $E_x[\rho]$ is the exchange energy of a spin-unpolarized system [30], and

$$E_x[\rho_{\uparrow\lambda}, \rho_{\downarrow\lambda}] = \lambda E_x[\rho_\uparrow, \rho_\downarrow] \tag{9}$$

where $\rho_{\sigma\lambda}(\mathbf{r}) = \lambda^3\rho_\sigma(\lambda\mathbf{r})$ is a uniformly-scaled density [31]. As a consequence of Eqs. 8 and 9, the GGA for exchange assumes the simple form

$$E_x^{GGA}[\rho] = \int d^3r\ \rho\epsilon_x(\rho)F_x(s), \tag{10}$$

where $\epsilon_x(\rho) = -3k_f/4\pi$, $k_f = (3\pi^2\rho)^{1/3}$ is the local Fermi wavevector, and $s = |\nabla\rho|/2k_f\rho$ is a dimensionless density gradient. Different GGA's for exchange correspond to different choices for the function $F_x(s)$.

Starting from the exchange-correlation energy functional, the exchange component can be picked out by uniform scaling to the high-density limit, i.e., [32]

$$E_x[\rho_\uparrow, \rho_\downarrow] = \lim_{\lambda\to\infty} \lambda^{-1} E_{xc}[\rho_{\uparrow\lambda}, \rho_{\downarrow\lambda}] \tag{11}$$

for a density whose ground-state wavefunction is non-degenerate. However, the valence electrons of a molecule are far from the high-density limit, so the contribution of Coulomb correlation to the atomization energy is comparable to that of exchange. Coulomb correlation (the tendency of any two electrons to stay apart because of the repulsive force between them) further lowers the electron-electron repulsion energy V_{ee}, and further stabilizes the molecule relative to the separated atoms.

If correlation is neglected, the only difference between Hartree-Fock and Kohn-Sham theory is the appearance of a *local* exchange potential $v_x^\sigma(\mathbf{r})$ in the latter theory. Recently a number of methods have been presented for the construction of this potential from orbitals, either exactly [33,34] or to a good approximation [35,36].

2. The ground-state energy and its exchange component

The ground-state energy of a Coulomb system can be expressed in terms of the one- and two-particle density matrices γ and Γ,

$$\begin{aligned}\gamma(\mathbf{r},\sigma,\mathbf{r}',\sigma') &= N\int d\sigma_2\ldots d\sigma_N, d^3r_2\ldots d^3r_N \\ &\times\ \psi^*(\mathbf{r},\sigma,\mathbf{r}_2,\sigma_2,\ldots,\mathbf{r}_N,\sigma_N)\psi(\mathbf{r}',\sigma',\mathbf{r}_2,\sigma_2,\ldots,\mathbf{r}_N,\sigma_N),\end{aligned} \tag{12}$$

$$\begin{aligned}\Gamma(\mathbf{r}_1,\sigma_1,\mathbf{r}_2,\sigma_2;\mathbf{r}_1',\sigma_1',\mathbf{r}_2',\sigma_2') &= N(N-1)\int d\sigma_3\ldots d\sigma_N, d^3r_3\ldots d^3r_N \\ &\times\ \psi^*(\mathbf{r}_1,\sigma_1,\mathbf{r}_2,\sigma_2,\mathbf{r}_3,\sigma_3,\ldots,\mathbf{r}_N,\sigma_N) \\ &\times\ \psi(\mathbf{r}_1',\sigma_1',\mathbf{r}_2',\sigma_2',\mathbf{r}_3,\sigma_3,\ldots,\mathbf{r}_N,\sigma_N),\end{aligned} \tag{13}$$

where $\psi(\mathbf{r}_1,\sigma_1,\mathbf{r}_2,\sigma_2,\ldots,\mathbf{r}_N,\sigma_N)$ denotes the ground-state wavefunction of the N-electron system of interest and $\mathbf{r}_i$ and σ_i are the spatial- and spin coordinates, respectively, of the electrons. Now the ground-state expectation value of the Hamiltonian is

$$\begin{aligned} E &= T+v+V_{ee} \\ &= -\frac{1}{2}\int d^3r d\sigma\ \Delta_{\mathbf{r}'}\gamma(\mathbf{r},\sigma,\mathbf{r}',\sigma)|_{\mathbf{r}=\mathbf{r}'} + \int d^3r d\sigma\ \gamma(\mathbf{r},\sigma,\mathbf{r},\sigma)v(\mathbf{r}) \\ &+ \frac{1}{2}\int d^3\mathbf{r}_1 d^3\mathbf{r}_2 d^3\mathbf{r}_1' d^3\mathbf{r}_2' d\sigma_1 d\sigma_2 d\sigma_1' d\sigma_2'\ \Gamma(\mathbf{r}_1,\sigma_1,\mathbf{r}_2,\sigma_2;\mathbf{r}_1',\sigma_1',\mathbf{r}_2',\sigma_2') \\ &\times \frac{\delta_{\sigma_1,\sigma_1'}\delta_{\sigma_2,\sigma_2'}\delta_{\mathbf{r}_1,\mathbf{r}_1'}\delta_{\mathbf{r}_2,\mathbf{r}_2'}}{|\mathbf{r}_1-\mathbf{r}_2|}. \end{aligned} \tag{14}$$

$v(\mathbf{r})$ denotes the external local potential. The diagonal part of γ, which appears in the term $\int d^3r d\sigma\ \gamma(\mathbf{r},\sigma,\mathbf{r},\sigma)v(\mathbf{r})$ in the expression of Eq. 14 for the energy, is equal to the spin density

$$\rho_\sigma(\mathbf{r}) = \gamma(\mathbf{r},\sigma,\mathbf{r},\sigma). \tag{15}$$

Wavefunction methods such as Configuration Interaction techniques, Coupled-Cluster, or Møller-Plesset perturbation theory are usually implemented by introducing a one-particle basis of orbitals. As a consequence, no advantage can be taken of the fact that the electron-electron repulsion operator is a bi-local operator. I.e., the basis-set representation of the Coulomb operator leads to four index quantities, whereas the real-space representation leads to a matrix with two indices, namely $\mathbf{r}_1$ and $\mathbf{r}_2$. In actual calculations the spin-averaged diagonal part of Γ, the so called pair density $P(\mathbf{r}_1,\mathbf{r}_2)$

$$P(\mathbf{r}_1,\mathbf{r}_2) = \int d\sigma_1 d\sigma_2\ \Gamma(\mathbf{r}_1,\sigma_1,\mathbf{r}_2,\sigma_2;\mathbf{r}_1,\sigma_1,\mathbf{r}_2,\sigma_2), \tag{16}$$

needs to be approximated[1]. Again, wavefunction methods lead to a representation of $P(\mathbf{r}_1,\mathbf{r}_2)$ in terms of four index quantities. Recent developments in density functional theory have shown that the relevant component of $P(\mathbf{r}_1,\mathbf{r}_2)$ can be accurately approximated in real space, since a number of important conditions are known, which must be satisfied by any real-space representation of $P(\mathbf{r}_1,\mathbf{r}_2)$. What is meant by the relevant part of $P(\mathbf{r}_1,\mathbf{r}_2)$ will be explained now. We note that the electron-electron interaction energy V_{ee} is given in terms of the pair density $P(\mathbf{r}_1,\mathbf{r}_2)$ by

$$V_{ee} = \frac{1}{2}\int d^3r_1 d^3r_2\ \frac{P(\mathbf{r}_1,\mathbf{r}_2)}{|\mathbf{r}_1-\mathbf{r}_2|}. \tag{17}$$

Variable substitution $\mathbf{r}_2 = \mathbf{r}_1+\mathbf{u}$ leads to

$$\begin{aligned} V_{ee} &= \frac{1}{2}\int d^3u\ \frac{\int d^3r_1\ P(\mathbf{r}_1,\mathbf{r}_1+\mathbf{u})}{u} \\ &= \frac{1}{2}\int_0^\infty 4\pi u^2\ du\ \frac{\int \frac{d\Omega_\mathbf{u}}{4\pi}\int d^3r_1\ P(\mathbf{r}_1,\mathbf{r}_1+\mathbf{u})}{u}. \end{aligned} \tag{18}$$

[1]The one-matrix γ also needs to be approximated. We will come back to this point in chapter 4.

This shows that only the system- and spherically-averaged pair density $P(u)$,

$$P(u) = \int \frac{d\Omega_\mathbf{u}}{4\pi}\int d^3r_1\ P(\mathbf{r}_1,\mathbf{r}_1+\mathbf{u}), \tag{19}$$

is needed to calculate V_{ee}.

2.1. Exchange energy

2.1.1. The exchange hole

In this section we introduce basic quantities in density functional theory such as the exchange hole and its system- and spherical-average. The definition of these quantities can readily be generalized to include electron correlation effects (see the following section). To keep the discussion as simple as possible, we focus on exchange. The exchange limit is probably the weakest point of all density functionals, i.e., we do not expect local or semi-local density functionals to work so well for exchange. Coulomb correlation (section 3), which deepens and narrows the exchange-correlation hole, is needed to improve the performance of these approximations.

The reader familiar with the details of density functional theory will know that the Hartree-Fock exchange energy is in general not the same as the exchange energy obtained from the exact functional for exchange, $E_x[\rho]$ with $\rho=\rho^{HF}$, because of the small difference between Hartree-Fock and Kohn-Sham orbitals. Likewise the pair density of the exchange-only Kohn-Sham determinant corresponding to ρ^{HF} will not be equal to the pair density of the Hartree-Fock determinant. In practice, however, the difference between $E_x[\rho^{HF}]$ and the Hartree-Fock exchange energy is often negligible [37], and for the sake of simplicity we do not distinguish between the Hartree-Fock exchange energy and the density functional exchange energy evaluated on the Hartree-Fock density, $E_x[\rho^{HF}]$. Furthermore, we do not distinguish between the Hartree-Fock pair density and the pair density of the Kohn-Sham determinant which yields ρ^{HF}.

In the Hartree-Fock approximation the two-particle density matrix Γ is that of a Slater determinant, which is given in terms of the one-matrix γ^{HF} by

$$\begin{aligned} \Gamma^{HF}(\mathbf{r}_1,\sigma_1,\mathbf{r}_2,\sigma_2;\mathbf{r}_1',\sigma_1',\mathbf{r}_2',\sigma_2') &= \gamma^{HF}(\mathbf{r}_1,\sigma_1,\mathbf{r}_1',\sigma_1')\gamma^{HF}(\mathbf{r}_2,\sigma_2,\mathbf{r}_2',\sigma_2') \\ &- \gamma^{HF}(\mathbf{r}_1,\sigma_1,\mathbf{r}_2',\sigma_2')\gamma^{HF}(\mathbf{r}_2,\sigma_2,\mathbf{r}_1',\sigma_1'), \end{aligned} \tag{20}$$

with

$$\gamma^{HF}(\mathbf{r},\sigma,\mathbf{r}',\sigma') = \sum_i^{occ}\varphi_i^*(\mathbf{r},\sigma)\varphi_i(\mathbf{r}',\sigma')\delta_{\sigma,\sigma'}, \tag{21}$$

where the sum runs over the occupied Hartree-Fock spin-orbitals $\varphi_i(\mathbf{r},\sigma)$. The Hartree-Fock pair density becomes

$$P^{HF}(\mathbf{r}_1,\mathbf{r}_2) = \rho^{HF}(\mathbf{r}_1)\rho^{HF}(\mathbf{r}_2) - \sum_\sigma \gamma^{HF}(\mathbf{r}_1,\sigma,\mathbf{r}_2,\sigma)\gamma^{HF}(\mathbf{r}_2,\sigma,\mathbf{r}_1,\sigma), \tag{22}$$

where $\rho(\mathbf{r}) = \sum_\sigma \rho_\sigma(\mathbf{r})$. The first term on the right hand side is the uncorrelated part of the pair density and the second term describes the exchange contribution. Dividing the

pair density by the electron density at the point $\mathbf{r}_1$, we obtain a quantity which describes the probability density for finding an electron at a point $\mathbf{r}_2$ given an electron at point $\mathbf{r}_1$:

$$\frac{P^{HF}(\mathbf{r}_1,\mathbf{r}_2)}{\rho^{HF}(\mathbf{r}_1)} = \rho^{HF}(\mathbf{r}_2) - \frac{1}{\rho^{HF}(\mathbf{r}_1)} \sum_\sigma \gamma^{HF}(\mathbf{r}_1,\sigma,\mathbf{r}_2,\sigma)\gamma^{HF}(\mathbf{r}_2,\sigma,\mathbf{r}_1,\sigma). \tag{23}$$

The second term on the right hand side accounts for a reduction in the probability density due to non-classical effects. To familiarize ourselves with this expression, we think of a two-electron system, with one doubly occupied spatial orbital. In this case the expression of Eq. 23 can be readily simplified to give

$$\frac{P^{HF}(\mathbf{r}_1,\mathbf{r}_2)}{\rho^{HF}(\mathbf{r}_1)} = \rho^{HF}(\mathbf{r}_2) - \frac{1}{2}\rho^{HF}(\mathbf{r}_2). \tag{24}$$

This shows that, if we assume that one electron is at position $\mathbf{r}_1$, then the probability density for finding a second electron at point $\mathbf{r}_2$ is independent of $\mathbf{r}_1$ and equal to half the electron density at $\mathbf{r}_2$. Both electrons are in the same orbital, and if one electron is assumed to be at position $\mathbf{r}_1$ it cannot be anywhere else in the system, so that the probability density is simply reduced by $\rho^{HF}(\mathbf{r}_2)/2$. In this simple example the hole does not follow the position of the electron labelled 1, i.e., the hole is independent of $\mathbf{r}_1$.

If more than one orbital is occupied, $P(\mathbf{r}_1,\mathbf{r}_2)/\rho(\mathbf{r}_1)$ in general becomes a function of $\mathbf{r}_1$ and $\mathbf{r}_2$. In cases where the two electrons have the same spin orientation and occupy different orbitals (which are assumed to be real functions), the hole becomes

$$\begin{aligned}\frac{P^{HF}(\mathbf{r}_1,\mathbf{r}_2)}{\rho^{HF}(\mathbf{r}_1)} = \rho^{HF}(\mathbf{r}_2) &- \frac{1}{\rho^{HF}(\mathbf{r}_1)}\Big[\varphi_1^2(\mathbf{r}_1,\sigma)\varphi_1^2(\mathbf{r}_2,\sigma) + \varphi_2^2(\mathbf{r}_1,\sigma)\varphi_2^2(\mathbf{r}_2,\sigma) \\ &+ 2\varphi_1(\mathbf{r}_1,\sigma)\varphi_2(\mathbf{r}_1,\sigma)\varphi_1(\mathbf{r}_2,\sigma)\varphi_2(\mathbf{r}_2,\sigma)\Big].\end{aligned} \tag{25}$$

The non-classical term of the probability distribution takes a more complicated form than in the previous example. The second term on the right hand side of Eq. 25 involves the probability density that an electron in the orbital φ_1 is at point $\mathbf{r}_1$ times the probability density that the second electron in the orbital φ_1 is at point $\mathbf{r}_2$. The third term on the right hand side involves a similar product except that φ_1 has been replaced by φ_2. The cross term in the above equation becomes important only in regions of space where there is a significant overlap between the orbitals φ_1 and φ_2. Everywhere else either the second or third term on the right hand side will dominate, so that the hole in the density will be localized in one of the orbitals. In regions of space where the cross terms are important, we obtain a hybrid hole [38], i.e., a hole which is localized in a hybrid orbital. An example of such a hybrid hole is shown in Fig. 9 of Ref. [39], where cuts through the exchange hole in the Ne atom are plotted. The reference electron is localized in the L shell and the exchange hole is a hybrid hole in the $2s$ and $2p$ orbitals. $P(\mathbf{r}_1,\mathbf{r}_2)/\rho(\mathbf{r}_1)$ is now a function of $\mathbf{r}_1$ and $\mathbf{r}_2$.

At this point it is natural to define the Hartree-Fock exchange hole $\rho_x^{HF}(\mathbf{r}_1,\mathbf{r}_2)$:

$$\rho_x^{HF}(\mathbf{r}_1,\mathbf{r}_2) = \frac{P^{HF}(\mathbf{r}_1,\mathbf{r}_2)}{\rho^{HF}(\mathbf{r}_1)} - \rho^{HF}(\mathbf{r}_2)$$

$$= -\frac{1}{\rho^{HF}(\mathbf{r}_1)} \sum_\sigma \gamma^{HF}(\mathbf{r}_1,\sigma,\mathbf{r}_2,\sigma)\gamma^{HF}(\mathbf{r}_2,\sigma,\mathbf{r}_1,\sigma). \tag{26}$$

This quantity describes the reduction in the electron density at point $\mathbf{r}_2$ due to the presence of an electron at $\mathbf{r}_1$. We expect that

$$\int d^3\mathbf{r}_2\ \rho_x^{HF}(\mathbf{r}_1,\mathbf{r}_2) = -1, \tag{27}$$

since the integrated reduction of the electron density should be one electron, to account for the fact that one electron is at $\mathbf{r}_1$. By making use of the idempotency of the one-particle density matrix of a Slater determinant, i.e.,

$$\begin{aligned}\int d^3r_2 d\sigma'\ \gamma(\mathbf{r}_1,\sigma,\mathbf{r}_2,\sigma')\gamma(\mathbf{r}_2,\sigma',\mathbf{r}_1,\sigma) &= \gamma(\mathbf{r}_1,\sigma,\mathbf{r}_1,\sigma) \\ &= \rho_\sigma(\mathbf{r}_1),\end{aligned} \tag{28}$$

we see that this is indeed the case. Furthermore, it is easy to read from the definition of Eq. 26 that

$$\rho_x^{HF}(\mathbf{r}_1,\mathbf{r}_2) \le 0. \tag{29}$$

An important property of the exchange hole (of a single determinant) is that the on-top value (i.e., $\mathbf{r}_1 = \mathbf{r}_2$) of the exchange hole is given exactly in terms of the spin density [40]. From Eq. 26 we obtain

$$\rho_x^{HF}(\mathbf{r}_1,\mathbf{r}_1) = -\frac{1}{\rho^{HF}(\mathbf{r}_1)} \sum_\sigma (\rho_\sigma^{HF}(\mathbf{r}_1))^2. \tag{30}$$

2.1.2. Local density approximation to the exchange hole

A simple approximation to the exact exchange hole should fulfill the properties of the exact exchange hole derived above. The correct on-top value and the non-positivity and normalization conditions ensure a qualitative agreement of approximate and exact exchange holes.

Before we introduce a model for the exchange hole, we derive a simplification which states that the exchange hole of a spin-polarized system can be expressed in terms of the exchange hole of a spin-unpolarized system [19]. From Eq. 26 we see that the exchange hole is the sum of a hole in the α- and another in the β-spin density:

$$\rho_x(\mathbf{r}_1,\mathbf{r}_1+\mathbf{u}) = \rho_{x\uparrow}(\mathbf{r}_1,\mathbf{r}_1+\mathbf{u}) + \rho_{x\downarrow}(\mathbf{r}_1,\mathbf{r}_1+\mathbf{u}), \tag{31}$$

where $\rho_{x\uparrow}(\mathbf{r}_1,\mathbf{r}_1+\mathbf{u}) = -\frac{1}{\rho(\mathbf{r}_1)}|\gamma(\mathbf{r}_1,\uparrow,\mathbf{r}_2,\uparrow)|^2$. The hole in the up-spin density $\rho_\uparrow(\mathbf{r})$ is essentially the exchange hole in a spin-unpolarized system with a density $\rho(\mathbf{r}) = 2\rho_\uparrow(\mathbf{r})$. An analogous result holds for the hole in the down-spin density, so that we have

$$\rho_x(\mathbf{r}_1,\mathbf{r}_1+\mathbf{u}) = c_1\rho_x([2\rho_\uparrow],\mathbf{r}_1,\mathbf{r}_1+\mathbf{u}) + c_2\rho_x([2\rho_\downarrow],\mathbf{r}_1,\mathbf{r}_1+\mathbf{u}). \tag{32}$$

The coefficients c_1 and c_2 are determined by Eq. 30 to be

$$c_1 = \rho_\uparrow(\mathbf{r}_1)/\rho(\mathbf{r}_1), \quad c_2 = \rho_\downarrow(\mathbf{r}_1)/\rho(\mathbf{r}_1). \tag{33}$$

The only system-dependent property of the above-listed properties of the exchange hole is the on-top value of the hole, which in turn can be expressed through the spin density. It is therefore reasonable to model the exchange hole in terms of the local spin density $\rho_\sigma(\mathbf{r})$. The exchange hole $\rho_x^{LSD}(\rho_\uparrow(\mathbf{r}_1),\rho_\downarrow(\mathbf{r}_1),\mathbf{r}_1,\mathbf{r}_1+\mathbf{u})$ of a homogeneous electron gas of spin density ρ_σ fulfills all the conditions given above, including the condition on the on-top value of the hole. Furthermore, the exchange hole of the homogeneous electron gas is analytically known. For a spin-unpolarized system we have

$$\rho_x^{LSD}(\rho/2,\rho/2,\mathbf{r}_1,\mathbf{r}_1+\mathbf{u}) = \frac{-3k_f}{2\pi^2u^2}\left(\frac{\sin(uk_f)}{(uk_f)^2}-\frac{\cos(uk_f)}{uk_f}\right)^2, \quad k_f=[3\pi^2\rho(\mathbf{r})]^{1/3}. \tag{34}$$

This model for the exchange hole yields a corresponding model for the pair density:

$$P^{LSD}(\mathbf{r}_1,\mathbf{r}_1+\mathbf{u}) = \rho(\mathbf{r}_1)\rho(\mathbf{r}_1+\mathbf{u}) + \rho(\mathbf{r}_1)\rho_x^{LSD}(\mathbf{r}_1,\mathbf{r}_1+\mathbf{u}). \tag{35}$$

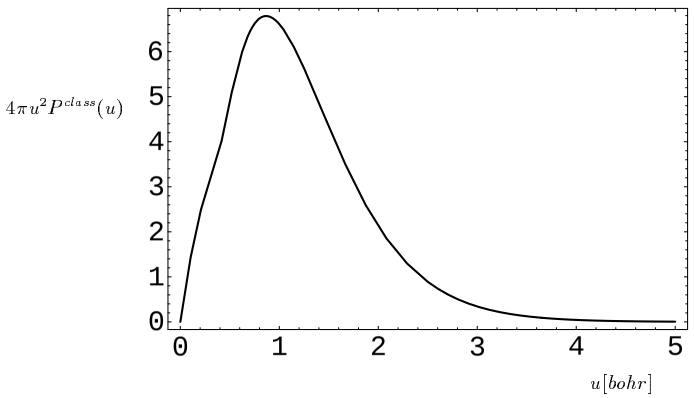

Figure 1. Uncorrelated contribution $P^{class}(u)$ to the system-and spherically-averaged pair density of the Ne atom.

We do not expect this approximation to describe the details of $P(\mathbf{r}_1,\mathbf{r}_1+\mathbf{u})$ as a function of both variables correctly, but in order to estimate the electron-electron interaction we only need the system- and spherically-averaged pair density $P(u)$,

$$\begin{aligned} P(u) &= \int\frac{d\Omega_{\mathbf{u}}}{4\pi}\int d^3r_1\ \rho(\mathbf{r}_1)\rho(\mathbf{r}_1+\mathbf{u}) \\ &+ \int\frac{d\Omega_{\mathbf{u}}}{4\pi}\int d^3r_1\ \rho(\mathbf{r}_1)\rho_x(\mathbf{r}_1,\mathbf{r}_1+\mathbf{u}) \\ &= P^{class}(u)+N\langle\rho_x\rangle(u), \end{aligned} \tag{36}$$

in which many fine details are washed away. N in this equation stands for the particle number. The first term on the right hand side is the classical or uncorrelated part of the pair density, which is straightforward to calculate as a functional of the electron density. The second or non-classical term, which is only approximately known as a functional of the density, will be the quantity we are concerned with. Fig. 1 shows the radial uncorrelated part of the pair density, i.e., $4\pi u^2P^{class}(u)$. This function gives the classical probability density to find an electron at a distance u from another electron. The shell structure of the Ne atom is still visible in this quantity. The shoulder at about $0.2a_0$ is due to the electrons in the K shell.

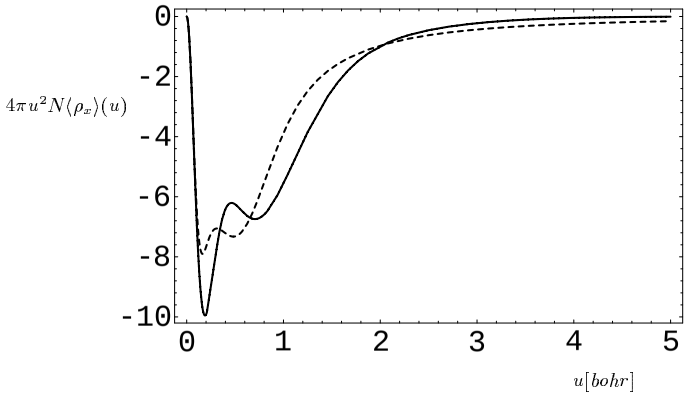

Figure 2. Comparison of the exact (solid line) and the LSD approximation (dashed line) to the system- and spherically-averaged exchange hole of the Ne atom.

In Fig. 2 the quantities $4\pi u^2N\langle\rho_x^{HF}\rangle(u)$ and $4\pi u^2N\langle\rho_x^{LSD}\rangle(u)$ are compared. $4\pi u^2N\langle\rho_x^{HF}\rangle(u)$ clearly shows the shell structure of the Ne atom, and the LSD approximation is in semiquantitative agreement with the Hartree-Fock result.

For intermediate u values on the length scale of the K shell (i.e., $u\in[0.05,0.15]$), the LSD exchange hole is not negative enough and the shell oscillation in $\langle\rho_x^{HF}(u)\rangle$ is only qualitatively reproduced. The same is true for the hole at intermediate u-values on the scale of the L shell. It is interesting to note that the shell oscillations are not averaged out in the spherical- and system-average. The explanation for this feature of the radial exchange hole is that, for small enough u, $\mathbf{r}$ and $\mathbf{r}+\mathbf{u}$ are in the $1s$ shell for all values of $\mathbf{r}$ inside the $1s$ shell, which leads to large negative contributions to the system-averaged hole. For $u>0.1a_0$, where $0.1a_0$ is roughly half the radius of the $1s$ shell, $\mathbf{r}$ and $\mathbf{r}+\mathbf{u}$ fall in different shells for a significant fraction of $r-$space, even if $\mathbf{r}$ is located in the $1s$ shell. Since the hole is basically localized in a certain shell, the contribution to the

system-averaged hole suddenly drops for $u > 0.1a_0$.

To understand the LSD underestimation of the depth of the hole at intermediate u values, we need to look at the local hole $\rho_x(\mathbf{r}, \mathbf{r}+\mathbf{u})$. In an atom the minimum value of $\rho_x^{HF}(\mathbf{r}, \mathbf{r}+\mathbf{u})$ as a function of $\mathbf{u}$ is shifted towards the nucleus (where the density is higher), whereas $\rho_x^{LSD}(\mathbf{r}, \mathbf{r}+\mathbf{u})$ has its minimum at $u = 0$. This different behavior of $\rho_x^{LSD}(\mathbf{r}, \mathbf{r}+\mathbf{u})$ and $\rho_x^{HF}(\mathbf{r}, \mathbf{r}+\mathbf{u})$ becomes particularly obvious if we look at a closed-shell system with two electrons, where $\rho_x^{HF}(\mathbf{r}, \mathbf{r}+\mathbf{u}) = -\rho(\mathbf{r}+\mathbf{u})/2$. This observation explains why $\langle\rho_x^{LSD}\rangle(u)$ is too shallow compared to the exact exchange hole at intermediate u-values, which in turn results in an underestimation of the magnitude of the exchange energy. The LSD exchange hole always 'follows' the electron at point $\mathbf{r}$, in the sense that the minimum of $\rho_x^{LSD}(\mathbf{r}, \mathbf{r}+\mathbf{u})$ is at $u = 0$. In the tail region the LSD and Hartree-Fock holes cross over and the LSD hole shows a slowly decaying tail. The LSD exchange hole has a power law decay as $u \to \infty$, which is unrealistic for systems with exponentially decaying densities. Thus, the LSD approximation predicts a hole in the electron density where there is no electron density. This long-range tail is tied via the normalization constraint on the exchange hole with the LSD hole being too shallow for intermediate u-values. (Note however that the large-u Friedel oscillations of the uniform-gas exchange hole, which have no counterpart in atoms and molecules, are properly washed away by the system- and spherical averaging.)

2.1.3. Exchange energy in terms of the exchange hole

Usually we are more interested in the energetics of the system than in the pair density and the hole. Therefore we decompose the electron-electron interaction energy into the contribution coming from the uncorrelated part of the pair density and the contribution coming from the hole around an electron. In the exchange-only approximation the

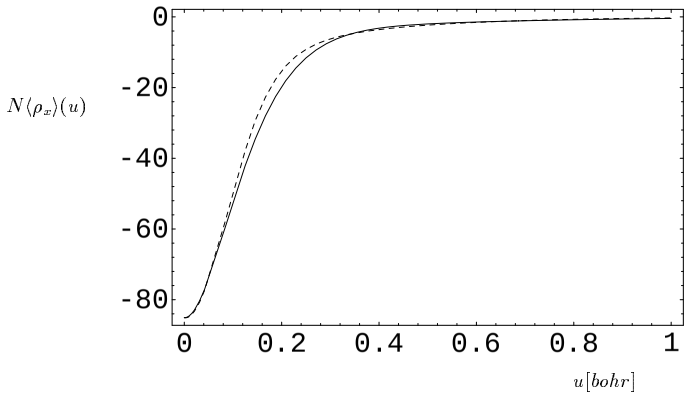

Figure 3. Exact (solid line) and LSD approximation (dashed line) to the system- and spherically-averaged exchange hole of the Ne atom. Unlike the correlation holes, these exchange holes have no electron-electron cusp at $u = 0$.

electron-electron interaction energy can be written as

$$\begin{aligned} V_{ee} &= 2\pi \int_0^\infty du\ uP(u) \\ &= 2\pi \int_0^\infty du\ uP^{class}(u) + 2\pi N \int_0^\infty du\ u\langle\rho_x\rangle(u). \end{aligned} \tag{37}$$

The second term on the right hand side gives the exchange energy, i.e.,

$$E_x = 2\pi N \int_0^\infty du\ u\langle\rho_x\rangle(u). \tag{38}$$

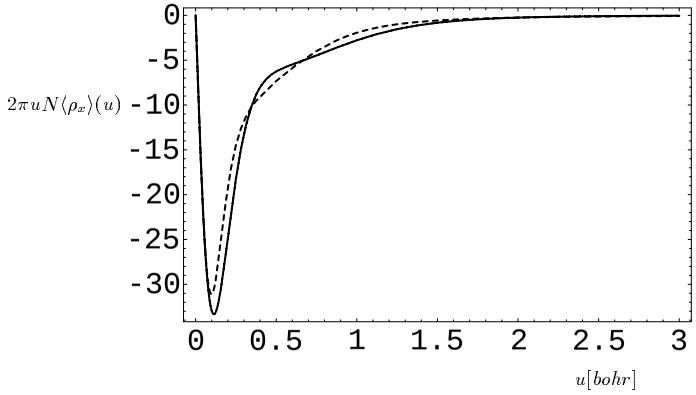

Figure 4. Exact (solid line) and LSD approximation (dashed line) to the weighted exchange hole or energy density $2\pi uN\langle\rho_x\rangle(u)$ in the Ne atom.

Since the second moment $4\pi\int_0^\infty du\ u^2\langle\rho_x\rangle(u) = -1$ is fixed by Eq. 27, the first moment or exchange energy of Eq. 38 becomes more negative when the hole becomes more localized about $u = 0$. Fig. 4 shows the integrand of the Hartree-Fock exchange energy, i.e., $2\pi uN\langle\rho_x^{HF}\rangle(u)$, and compares it with the corresponding LSD approximation $2\pi uN\langle\rho_x^{LSD}\rangle(u)$. $2\pi uN\langle\rho_x\rangle(u)$ is a more interesting quantity to study than the hole itself (see Fig. 3), because the hole is highly dominated by contributions from the core electrons at short u-values and this contribution gets suppressed by the factor u. We will refer to $2\pi uN\langle\rho_x\rangle(u)$ as the weighted hole. The above-discussed failure of the LSD hole to describe the intermediate region of the hole in the K and in the L shell leads to an underestimation of the magnitude of the exchange energy. The Hartree-Fock exchange energy of the Ne atom is -12.108 hartree, whereas the LSD exchange energy is -11.033 hartree.

2.1.4. The LSD approximation for the exchange contribution to atomization energies

The effect that the LSD exchange hole follows the reference electron contributes to the differential error in the exchange energy between a molecule and the separated atoms.

Table 1
Exchange contribution ΔE_x to the atomization energy, evaluated exactly and within the LSD approximation on the LSD densities. $\Delta E_x = E_x(atoms) - E_x(molecule)$. The mean absolute errors (m.a.e.) are also reported.

System	ΔE_{xc} exact	E_x molecule	E_x atoms	ΔE_x exact	E_x^{LSD} molecule	E_x^{LSD} atoms	ΔE_x^{LSD}
H_2	.090	-.648	-.597	.051	-.559	-.513	.045
CH_4	.468	-6.536	-6.215	.320	-5.864	-5.476	.388
H_2O	.262	-8.876	-8.736	.140	-8.075	-7.845	.231
HF	.160	-10.343	-10.253	.090	-9.438	-9.286	.152
m.a.e.	-	-	-	-	.617	.670	.057
CO	.213	-13.229	-13.159	.070	-11.998	-11.780	.217
N_2	.137	-13.035	-13.088	-.053	-11.824	-11.715	.109
NO	.106	-14.616	-14.682	-.066	-13.300	-13.189	.112
O_2	.099	-16.224	-16.277	-.053	-14.805	-14.663	.142
m.a.e.	-	-	-	-	1.294	1.465	.170

The minimum in the exact exchange hole in a homonuclear diatomic molecule is to a lesser extent displaced towards one or the other nuclei than is that of the exact exchange hole in the separated atoms. In the midbond region, the two nuclei compete for the electron density and the hole becomes more isotropic compared to the hole of an atom. The LSD approximation neglects the displacement of the hole completely and therefore introduces a differential error in the exchange energy. In general as shown in Table 1 the exchange energy of the molecule is better described within the LSD approximation than the exchange energy of the separated atoms. The data compiled in this table have been obtained with the CADPAC program [41]. Self-consistent local spin density calculations have been carried out, and the exact exchange results have been obtained by evaluating the exchange energy of the Kohn-Sham determinant. Details of the calculations can be found in the appendix.

Another way of explaining the better performance of the LSD approximation for molecules as opposed to the separated atoms goes as follows. The density gradients in the molecule tend to be smaller than the density gradients in the separated atoms, so that an approximation which neglects the gradient (and all higher derivatives) of the density works better for molecules. LSD fails to make the exchange energy negative enough. This failure, which is more pronounced in the atom, leads to an LSD overestimation of the binding energy at the exchange-only level. Table 1 shows that the LSD approximation to ΔE_x does not compare well with the exact ΔE_x, especially for the multiply-bonded molecules collected in the bottom half of the table. However, ΔE_x^{LSD} is a much better approximation to the exact exchange-correlation energy difference ΔE_{xc}. ΔE_{xc} is obtained by subtracting $\Delta(E^{LSD} - E_{xc}^{LSD})$ from the experimental atomization energies.

2.2. Improving the model for the exchange hole by including the gradient of the density

2.2.1. The gradient expansion of the exchange hole

To improve the accuracy of the LSD exchange hole, we seek a model for the exchange hole which is able to account for its anisotropy around the position of the reference electron. The above-described local spin density approximation to the one-particle density matrix emerges naturally as the zeroth-order approximation from the semiclassical expansion [2] of the one-particle density matrix. In this semiclassical expansion, the one-particle density matrix is expanded in powers of $\hbar$ and subsequently the external potential in this expansion is eliminated in favor of the electron density and its derivatives. The resulting gradient expansion approximation $\gamma^{GEA}(\mathbf{r}_1, \sigma, \mathbf{r}_1+\mathbf{u}, \sigma)$ is then used to construct the GEA hole. The resulting expression for ρ_x^{GEA} is further simplified by making use of the fact that, in the system-average, Laplacian terms can be transformed to gradient terms, i.e., $\int d^3r f(\rho(\mathbf{r}))\Delta\rho(\mathbf{r}) = -\int d^3r f'(\rho(\mathbf{r}))(\nabla\rho(\mathbf{r}))^2$. The important consequence of this modification of the GEA exchange hole is that the modified hole is no longer an approximation to the local hole but only to the system-averaged hole. Therefore the system-averaged exchange hole introduced in section 2 is the quantity which gets approximated in the present formalism. Note, however, that the integration by parts leaves the terms of zeroth and first order in the density gradient unchanged. The resulting hole for a spin-unpolarized system is [2,16]

$$\begin{aligned}\rho_x^{GEA}(\mathbf{r}, \mathbf{r}+\mathbf{u}) &= -\frac{1}{2}\rho(\mathbf{r}) \\ &\times \left[J(z) + \tilde{L}(z)\ \hat{\mathbf{u}}\cdot\mathbf{s}(\mathbf{r}) - \tilde{M}(z)\,(\hat{\mathbf{u}}\cdot\mathbf{s}(\mathbf{r}))^2 - \tilde{N}(z)s^2(\mathbf{r})\right],\end{aligned} \tag{39}$$

where

$$\mathbf{s}(\mathbf{r}) = \frac{\nabla n(\mathbf{r})}{2k_f(\mathbf{r})n(\mathbf{r})}, \tag{40}$$

and $J, \tilde{L}, \tilde{M}$, and $\tilde{N}$ are given by

$$\begin{aligned} J &= 72\frac{[4+z^2-(4-z^2)\cos(z)-4z\sin(z)]}{z^6}, \\ \tilde{L} &= 12\frac{[2-2\cos(z)-z\sin(z)]}{z^3}, \\ \tilde{M} &= \frac{1}{3}\frac{[\sin(z)-z\cos(z)]}{z}, \\ \tilde{N} &= \frac{[8-(8-4z^2)\cos(z)-(8z-z^3)\sin(z)]}{z^4}, \end{aligned} \tag{41}$$

with $z = 2k_f(\mathbf{r})u$. The zeroth-order term in $\mathbf{s}(\mathbf{r})$ gives the exchange hole in the LSD approximation, and the first-order term in $\mathbf{s}(\mathbf{r})$ ensures that the minimum in the hole is

shifted towards the high-density side of the reference electron, i.e., towards $\nabla\rho(\mathbf{r})$. To first order in u we have

$$\rho_x^{GEA}(\mathbf{r}, \mathbf{r}+\mathbf{u}) = -\frac{1}{2}\rho(\mathbf{r}+\mathbf{u}), \tag{42}$$

which is the correct behavior of the exchange hole. Note that this first-order term does not contribute to the system-averaged hole for systems where the density gradient $\nabla\rho(\mathbf{r})$ at each point in the system can be mapped onto its negative by a symmetry transformation, such as the H_2 molecule or any spherical atom.

The quadratic term in $\mathbf{u}$ does not cause a displacement of the minimum of the hole but does modify the angle dependence of the hole.

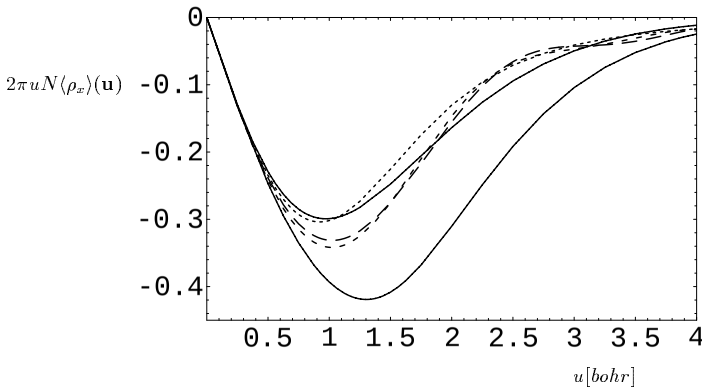

Figure 5. Angle-resolved weighted system-averaged exchange holes for H_2. The solid curves represent the exact results for $\hat{\mathbf{u}} \perp \hat{\mathbf{z}}$ (upper curve) and for $\hat{\mathbf{u}}||\hat{\mathbf{z}}$ (lower curve), the dotted curve shows the LSD result, and the dashed curves are the GEA for $\hat{\mathbf{u}} \perp \hat{\mathbf{z}}$ (long dashes) and $\hat{\mathbf{u}}||\hat{\mathbf{z}}$ (short dashes). The z-axis is the bond axis.

To investigate the GEA hole and its dependence on the orientation of $\mathbf{u}$, we define the system-averaged hole $\langle\rho_x\rangle(\mathbf{u})$ as the system- (but not spherical) average of the exchange hole:

$$\langle\rho_x\rangle(\mathbf{u}) = \frac{1}{N}\int d^3r\,\rho(\mathbf{r})\rho_x(\mathbf{r}, \mathbf{r}+\mathbf{u}). \tag{43}$$

The system of interest is now the H_2 molecule at the experimental equilibrium bond length of $1.401a_0$. In Fig. 5 a comparison is made of the GEA and the exact holes weighted by

$2\pi uN$. A fuller account of both the GEA and GGA system-averaged hole calculations appears in Ref. [42]. The weighted system-averaged hole in the LSD approximation, which is independent of $\hat{\mathbf{u}}$, is also shown. The orientation of $\hat{\mathbf{u}}$ is chosen such that $\hat{\mathbf{u}}||\hat{\mathbf{z}}$ and $\hat{\mathbf{u}} \perp \hat{\mathbf{z}}$, where the z-axis is the bond axis. As already mentioned, the linear term in $\mathbf{s}$ does not contribute to the system average of the exchange hole for this system. If we compare the GEA curves along the different directions, we observe a small splitting which can be traced back to the term quadratic in $\mathbf{u}\cdot\mathbf{s}$ in Eq. 39. The deepening of the weighted GEA hole compared to the weighted LSD hole must be attributed to the term quadratic in $\mathbf{s}$. Note that $\langle\rho_x\rangle(\mathbf{u})$ is independent of $\hat{\mathbf{u}}$ for spherical atoms, since there is no distinguished direction in such a system. The GEA hole reproduces part of the angle dependence of the

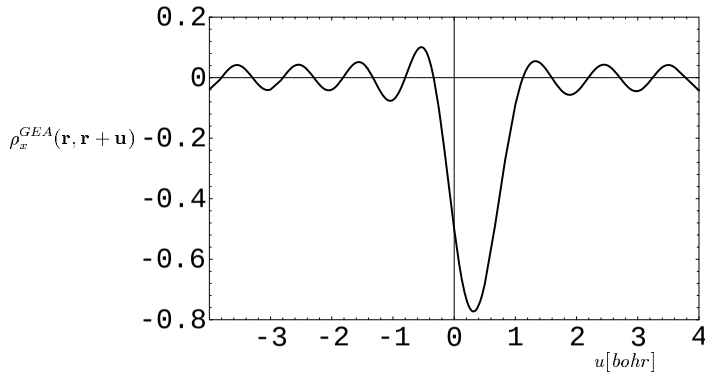

Figure 6. The GEA hole for $s = 1$ and $\rho = 1$, plotted along the direction of $\mathbf{s}$, i.e., $\hat{\mathbf{u}}||\hat{\mathbf{s}}$.

exact hole. The hole along the bond axis is slightly deeper than the hole perpendicular to the bond axis for intermediate u values, i.e., for $u < 1.5a_0$. For $u > 1.5a_0$ the GEA holes oscillate around each other, as a consequence of unphysical oscillations in the GEA hole as u becomes large. Also for $u > 1.5a_0$, the GEA curves are no longer bracketed by the exact angle-resolved holes, which are the solid curves in Fig. 5. The exact angular variation of the weighted exchange hole is much bigger than predicted by the GEA expansion.

To illustrate the unrealistic large-u behavior of the GEA to the exchange hole, we plot the hole for $\rho = 1$, and $s = 1/2$ along the direction of $\mathbf{s}$ in Fig 6. The GEA hole is shifted toward the high-density side, as expected. Unphysical features of the GEA hole, visible in Fig. 6 but not in the system-averaged holes of Fig. 5, are that it is not always negative and that it shows a long-range undamped oscillation which leads to a violation of the

normalization condition. These unphysical features of the GEA hole arise because each successive term in the gradient expansion, while improving the hole at small u, worsens it at large u [43]. They are responsible for an order-of-limits dependence [7,44] of the gradient coefficient C_x in Eq. 4.

2.2.2. The exchange hole in the generalized gradient approximation

In view of the findings in the previous section, we construct a GGA by modifying the large-u behavior of the GEA hole in such a way that the modified hole does not become positive and that it is normalized, i.e., we restore the exact conditions of Eqs. 27 and 29. This is achieved by the so-called real-space cutoff procedure [16–19]. The GEA hole as a function of $\mathbf{u}$ is set to zero if it becomes positive, and it is also set to zero for $u > u_c$, where the radial cutoff u_c is chosen such that the normalization condition for the exchange hole is satisfied. Furthermore, the GEA exchange hole is modified so that the long-range

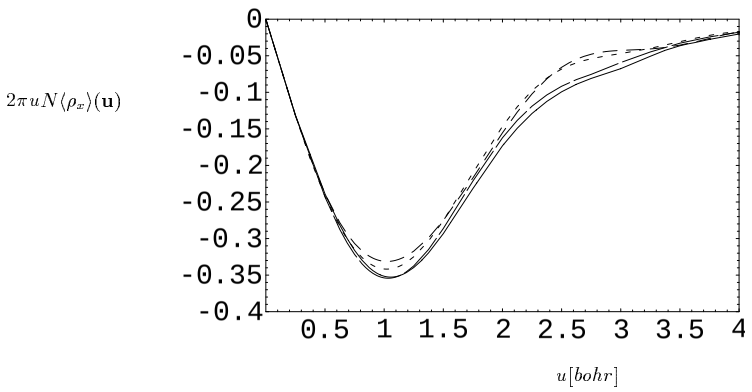

Figure 7. Comparison of the angle-dependent quantity $2\pi u N\langle\rho_x\rangle(\mathbf{u})$ for H_2 in GEA and GGA for $\hat{\mathbf{u}}||\hat{\mathbf{z}}$ (shortest and longest dashes, respectively) and $\hat{\mathbf{u}} \perp \hat{\mathbf{z}}$ (intermediate dashed and solid line, respectively).

oscillations are damped by a factor such as

$$\frac{1}{[1+(0.13z)^3]}, \tag{44}$$

which multiplies the terms in the GEA hole which depend on $\mathbf{s}$. In formulas,

$$\rho_x^{GGA}(\mathbf{r},\mathbf{r}+\mathbf{u}) \;=\; \Theta(u_c(\mathbf{r})-u)\;\Theta(-\tilde{\rho}_x^{GEA}(\mathbf{r},\mathbf{r}+\mathbf{u}))\;\tilde{\rho}_x^{GEA}(\mathbf{r},\mathbf{r}+\mathbf{u}), \tag{45}$$

where the damped GEA hole $\tilde{\rho}_x^{GEA}(\mathbf{r},\mathbf{r}+\mathbf{u})$ is given by

$$\begin{aligned}\tilde{\rho}_x^{GEA}(\mathbf{r},\mathbf{r}+\mathbf{u}) \;&=\; -\frac{1}{2}\rho(\mathbf{r})\times\Bigg[J(z)\\ &+\; \frac{1}{[1+(0.13z)^3]}\left\{\tilde{L}(z)\;\hat{\mathbf{u}}\cdot\mathbf{s}(\mathbf{r})-\tilde{M}(z)\,(\hat{\mathbf{u}}\cdot\mathbf{s}(\mathbf{r}))^2-\tilde{N}(z)s^2(\mathbf{r})\right\}\Bigg].\end{aligned} \tag{46}$$

(Depictions of the GGA exchange hole, without damping or system averaging, have

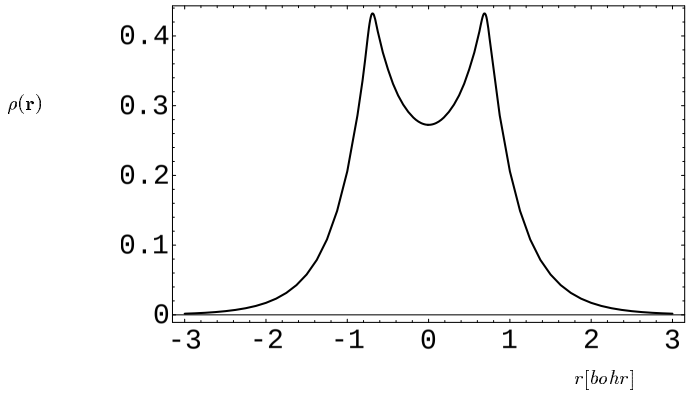

Figure 8. The electron density in H_2 along the bond axis.

been given by Slamet and Sahni [45].) With this GGA model for the exchange hole, we evaluate the energy integral of Eq. 38, yielding a numerically-defined function $F_x(s)$ for Eq. 10, to which we fit an analytic form [16,17,19]. This and other choices for $F_x(s)$ are plotted in Refs. [46] and [47].

In Fig. 7 we compare GGA to GEA for the angle-dependent weighted hole. For small values of u we again find the correct ordering of the curves parallel and perpendicular to the bond axis. The cutoff procedure correctly removes the long-range oscillations in the GEA hole and leads to a deeper hole at $u \approx 2.5$.

To address the question why the angle dependence in the GEA and in the GGA expansion is underestimated, we plot the electron density of the H_2 molecule along the z-axis in Fig. 8. For this unpolarized two-electron system, the exact exchange hole is simply given by $-\rho(\mathbf{r}_1+\mathbf{u})/2$. We place the reference electron at some point between the left nucleus and the bond center. A large portion of the exact hole is localized at the right nucleus, making the system-averaged hole $\langle\rho_x\rangle(\mathbf{u})$ much deeper for $\mathbf{u}$ parallel to the bond axis

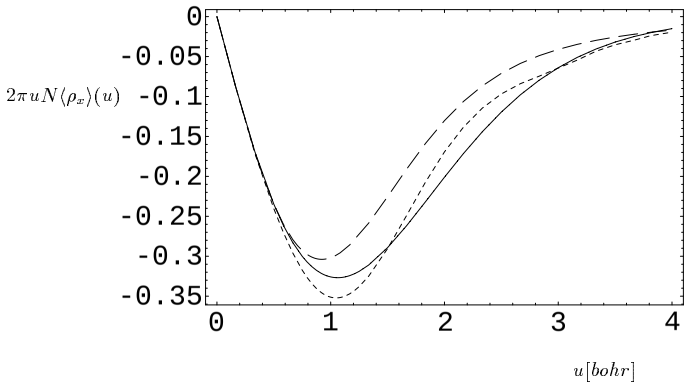

Figure 9. System- and spherically-averaged exchange holes for H_2 weighted by $2\pi uN$ in LSD (long dashes) and PW91 (short dashes). The solid curve represents the exact result.

than for **u** perpendicular to this axis. GEA and GGA, which use only information about the density and the gradient of the density, do not recognize and so miss this effect. GGA for exchange already contains correlation effects in the sense that it leads to an exchange hole which is more localized at the nearer nucleus. The GGA exchange error which shows up in the molecule is not a limitation of one particular GGA, but of the restricted ansatz for any GGA, which uses only the density and the gradient of the density. The exchange hole in this system is not really a semi-local quantity, and the degree of non-semi-locality is bigger in the H_2 molecule than in the separated atoms.

To see what the consequences for the exchange energy of the H_2 molecule are, we plot the weighted system- and spherically-averaged exchange holes in LSD and GGA and compare them with the exact result in Fig. 9. GGA gives a much better description of the hole than does LSD. The GGA hole is more realistic than the LSD hole for intermediate u values, and the unrealistic long-range decay of the LSD hole is suppressed.

2.2.3. Change in the spherically- and system-averaged hole upon breaking of the bond

To investigate the impact of the various approximations on the binding energy of the H_2 molecule, we introduce a differential exchange hole $\Delta\langle\rho_x\rangle(u)$, which describes the change in the exchange hole upon atomization of the molecule:

$$-\Delta\langle\rho_x\rangle(u) = \langle\rho_x\rangle_{H_2}(u) - \langle\rho_x\rangle_{2H}(u). \tag{47}$$

In Fig. 10 we compare the weighted differential spherically- and system-averaged holes in LSD and GGA with the exact result. The electron density becomes more compact upon bond formation, so that the hole becomes deeper for small u-values. Furthermore,

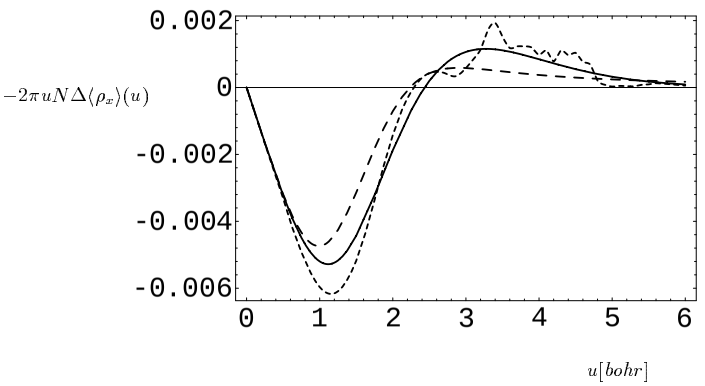

Figure 10. Differential spherically-and system-averaged holes upon atomization of H_2. The solid line represents the exact result, the long dashes show LSD, and the short dashed line is the GGA curve.

the density falls off faster in the molecule than in the separated atoms, so that the corresponding exchange holes show the same behavior. GGA clearly reproduces the exact curve much better than LSD. As in Fig.9 we again find that the weighted hole in the GGA oscillates around the exact curve, so that integration gives a value of the exchange energy difference of 0.0359 hartree in close agreement with the exact value of 0.0336 hartree. The exchange energy difference at the LSD level is 0.0294 hartree. The non-smooth features of the GGA curve for $u \in [3.5, 5]$ are due in part to numerical problems in the integration scheme which result from the normalization cutoffs.

We find that GGA underestimates the angle dependence of the system-averaged hole. However, it gives a good approximation to the system- and spherically averaged hole.

2.2.4. The PW91 approximation for the exchange contribution to atomization energies

The above analysis of the GGA hole suggests that the exchange energy of the separated atoms may be better approximated within a semi-local density functional than is the exchange energy of the molecule. Table 2 shows that this is indeed the case for the multiply-bonded molecules in the bottom half of the table: The PW91 GGA overestimates the magnitude of the exchange energy of the molecule by about 0.7%, while the corresponding error for the separated atoms is about 0.0%. The exact exchange hole in the molecule must be somewhat more delocalized than the PW91 exchange hole. Thus the general trend is reversed compared to LSD, which works better for the molecule than for the separated atoms. The total exchange energies as well as the differential exchange energies are significantly improved within GGA.

Table 2
Exchange contribution ΔE_x to the atomization energy, evaluated exactly and in the PW91 approximation of Refs. [17–19], on the LSD densities. The mean absolute errors (m.a.e.) are also reported.

System	E_x molecule	E_x atoms	ΔE_x exact	E_x^{PW91} molecule	E_x^{PW91} atoms	ΔE_x^{PW91}	ΔE_x^{LSD}
H_2	-.648	-.597	.051	-.641	-.589	.052	.045
CH_4	-6.536	-6.215	.320	-6.521	-6.185	.336	.388
H_2O	-8.876	-8.736	.140	-8.919	-8.732	.187	.231
HF	-10.343	-10.253	.090	-10.395	-10.271	.124	.152
m.a.e.	-	-	-	.029	.015	.025	.057
CO	-13.229	-13.159	.070	-13.309	-13.151	.158	.217
N_2	-13.035	-13.088	-.053	-13.123	-13.058	.065	.109
NO	-14.616	-14.682	-.066	-14.729	-14.672	.057	.112
O_2	-16.224	-16.277	-.053	-16.361	-16.287	.074	.142
m.a.e.	-	-	-	.104	.014	.114	.170

3. Exchange-correlation energy at full coupling strength

As already mentioned, the definition of quantities such as the exchange hole can readily be generalized if electron correlation is considered in addition to exchange effects. However, the approximations for the exchange-correlation holes become much more involved than those for the exchange holes. The exchange-correlation hole at full coupling strength[2] is defined in terms of the exact pair density of the interacting system by

$$\rho_{xc,\lambda=1}(\mathbf{r}_1,\mathbf{r}_2) \;=\; \frac{P(\mathbf{r}_1,\mathbf{r}_2)}{\rho(\mathbf{r}_1)} - \rho(\mathbf{r}_2). \tag{48}$$

The potential energy of exchange and correlation is then

$$E_{xc,\lambda=1} = \frac{1}{2}\int d^3r\ \rho(\mathbf{r}) \int d^3u\ \rho_{xc,\lambda=1}(\mathbf{r},\mathbf{r}+\mathbf{u})/u. \tag{49}$$

To successfully model the exchange-correlation hole, we need to know relevant properties of this hole to be included in the model. For example, it is easily shown that the sum rule which holds for the exchange hole is also a constraint on the exchange-correlation hole, i.e.,

$$\int d^3u\ \rho_{xc,\lambda=1}(\mathbf{r},\mathbf{r}+\mathbf{u}) = -1. \tag{50}$$

In the preceding section we saw that the on-top value of the exchange hole can be simply expressed in terms of the spin density. For a correlated system there is no such exact relation between the on-top value of the hole and the local spin density [48]. However,

[2]For the definition of exchange-correlation holes at other values of the coupling constant λ, we refer to the following section.

it has been demonstrated that the on-top value of the exchange-correlation hole as a function of the local density shows a nearly universal behavior [49], and thus to a good approximation can be transferred from the uniform electron gas to real systems. Furthermore the behavior of the exchange-correlation hole $\rho_{xc,\lambda=1}(\mathbf{r},\mathbf{r}+\mathbf{u})$ for small values of u is determined by the on-top value of the hole through the cusp condition

$$\frac{\partial}{\partial u}\int \frac{d\Omega_{\mathbf{u}}}{4\pi}\rho_{xc,\lambda}(\mathbf{r},\mathbf{r}+\mathbf{u})|_{u=0} = \lambda\left[\rho_{xc,\lambda}(\mathbf{r},\mathbf{r}) + \rho(\mathbf{r})\right]. \tag{51}$$

The exchange hole ($\lambda = 0$) of course has no cusp. The cusp also vanishes in the strongly-interacting limit ($\lambda \to \infty$), where $\rho_{xc,\lambda}(\mathbf{r},\mathbf{r}+\mathbf{u}) \to -\rho(\mathbf{r})$; the singularity of the Coulomb interaction λ/u as $u \to 0$ is not by itself sufficient to achieve the latter condition at finite λ. The PW91 model for the exchange-correlation hole respects all constraints discussed above and gives a realistic description of the system-averaged exchange-correlation hole.

For additional pictures of the exchange hole ρ_x and the exchange-correlation hole $\rho_{xc,\lambda=1}$, see Refs. [38,42]

4. Coupling-constant integration

In the preceding sections we discussed density functional models for the exchange hole and the exchange-correlation hole at full coupling strength. However, to evaluate the total energy $E = T + V_{ee} + v$ of an interacting system we also need to approximate the kinetic energy contribution. To this purpose the kinetic energy is written as the kinetic energy T_s of a non-interacting system which has the same density as the interacting system, plus a correction term T_c which accounts for the kinetic energy due to electron correlation. In this section we explain how this non-interacting system is defined and how the corresponding T_c is calculated [50,51,8]. We define a modified Hamiltonian

$$H_\lambda = T + \lambda V_{ee} + v_\lambda, \tag{52}$$

where the electron-electron repulsion operator is multiplied by the coupling constant λ. The $\lambda-$dependent potential v_λ, which is identical to the Coulomb potential of the nuclei at $\lambda = 1$, is added to keep the density fixed and equal to the physical spin density for all values of λ. For $\lambda = 0$ we obtain the Kohn-Sham non-interacting Hamiltonian, and for $\lambda = 1$ we obtain the physical Hamiltonian. Obviously we have

$$\begin{aligned} E &= \langle\psi_{\lambda=1}|H_{\lambda=1}|\psi_{\lambda=1}\rangle \\ &= \langle\psi_{\lambda=0}|H_{\lambda=0}|\psi_{\lambda=0}\rangle + \int_0^1 d\lambda \frac{d\langle\psi_\lambda|H_\lambda|\psi_\lambda\rangle}{d\lambda}, \end{aligned} \tag{53}$$

where ψ_λ is the ground state of H_λ. From the Hellmann-Feynman theorem it follows that

$$\frac{d\langle\psi_\lambda|H_\lambda|\psi_\lambda\rangle}{d\lambda} \;=\; \frac{1}{2}\int d^3r d^3r' \frac{P_\lambda(\mathbf{r},\mathbf{r}')}{|\mathbf{r}-\mathbf{r}'|} + \int d^3r \rho(\mathbf{r})\frac{d}{d\lambda}v_\lambda. \tag{54}$$

$P_\lambda(\mathbf{r},\mathbf{r}')$ is the pair density calculated from ψ_λ. Furthermore we have

$$\langle\psi_{\lambda=0}|H_{\lambda=0}|\psi_{\lambda=0}\rangle = T_s + \int d^3r\ \rho(\mathbf{r})v_{\lambda=0}(\mathbf{r}). \tag{55}$$

T_s is the kinetic energy of a non-interacting ($\lambda = 0$) ground-state wavefunction which yields the exact density $\rho(\mathbf{r})$ of the interacting system. From Eqs. 53, 54, and 55, we find

$$E = T_s + \int d^3r\ \rho(\mathbf{r})v(\mathbf{r}) + \frac{1}{2}\int_0^1 d\lambda \int d^3r d^3r'\ \frac{P_\lambda(\mathbf{r},\mathbf{r}')}{|\mathbf{r}-\mathbf{r}'|}. \tag{56}$$

The λ -dependent pair density is split up into a λ-independent classical term and the λ -dependent exchange-correlation hole $\rho_{xc,\lambda}(\mathbf{r},\mathbf{r}')$:

$$\frac{1}{2}\int d^3r d^3r' \frac{P_\lambda(\mathbf{r},\mathbf{r}')}{|\mathbf{r}-\mathbf{r}'|} = \frac{1}{2}\int d^3r d^3r'\ \frac{\rho(\mathbf{r})\rho(\mathbf{r}')}{|\mathbf{r}-\mathbf{r}'|} + \frac{1}{2}\int d^3r d^3r'\ \frac{\rho(\mathbf{r})\rho_{xc,\lambda}(\mathbf{r},\mathbf{r}')}{|\mathbf{r}-\mathbf{r}'|}. \tag{57}$$

Thus we obtain [50,51,8]

$$E = T_s + \int d^3r\ \rho(\mathbf{r})v(\mathbf{r}) + \frac{1}{2}\int d^3r d^3r'\ \frac{\rho(\mathbf{r})\rho(\mathbf{r}')}{|\mathbf{r}-\mathbf{r}'|} + \int_0^1 d\lambda\ E_{xc,\lambda}, \tag{58}$$

where

$$E_{xc,\lambda} = \frac{1}{2}\int d^3r d^3r'\ \frac{\rho(\mathbf{r})\rho_{xc,\lambda}(\mathbf{r},\mathbf{r}')}{|\mathbf{r}-\mathbf{r}'|}. \tag{59}$$

The important result of Eq. 58 shows that the kinetic energy contribution T_c to the correlation energy can be deduced from the λ-dependence of the pair density, and so made to "look like" a potential energy. At the $\lambda = 0$ end of the coupling-constant integration $\rho_{xc,\lambda}(\mathbf{r},\mathbf{r}')$ reduces to the exchange hole, and at $\lambda = 1$ to the exchange-correlation hole at full coupling strength. The exchange hole is more shallow and less centered around its electron than is the exchange-correlation hole at $\lambda = 1$. When the interaction is turned on, the hole around an electron becomes deeper and the sum rule ensures that the hole becomes more short-ranged. For the H_2 molecule we saw that the exchange hole extends over the entire molecule. For non-zero λ-values, the "left-right" correlation of the electrons ensures that the exact exchange-correlation hole becomes more localized around its electron. (When one electron is to the left of the bond midpoint, the other is very probably to the right.)

The exchange-correlation energy E_{xc} of density functional theory is now defined by

$$E_{xc} = \int_0^1 d\lambda\ E_{xc,\lambda}, \tag{60}$$

and its kinetic energy contribution is

$$T_c = E_{xc} - E_{xc,\lambda=1} = E_c - E_{c,\lambda=1}. \tag{61}$$

The Euler equation for the expression of Eq. 58 is

$$\mu_\sigma = \frac{\delta E}{\delta\rho_\sigma(\mathbf{r})} = \frac{\delta T_s}{\delta\rho_\sigma(\mathbf{r})} + v(\mathbf{r}) + \int d^3r' \frac{\rho(\mathbf{r}')}{|\mathbf{r}-\mathbf{r}'|} + \frac{\delta E_{xc}}{\delta\rho_\sigma(\mathbf{r})}. \tag{62}$$

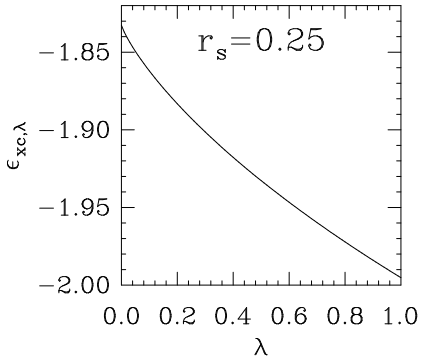

Figure 11. The λ-dependent exchange-correlation energy per particle of a uniform electron gas at a high density, $r_s = 0.25$ *bohr*, typical of core electrons. (Energy in hartrees).

This equation can be interpreted as the Euler equation of an independent-particle (Kohn-Sham) problem with local potential

$$v^\sigma_{eff}(\mathbf{r}) = v(\mathbf{r}) + \int d^3r' \frac{\rho(\mathbf{r}')}{|\mathbf{r}-\mathbf{r}'|} + \frac{\delta E_{xc}}{\delta\rho_\sigma(\mathbf{r})}, \tag{63}$$

as in Eq. 1.

Usually E_{xc} is approximated directly, starting from an electron gas of uniform or slowly-varying density. The λ-dependence of a given approximation to the integrated quantity E_{xc} can be extracted from $E_{xc}[\rho]$ via the scaling relation[31,52]

$$E_{xc,\lambda}[\rho] = \frac{d}{d\lambda}\left(\lambda^2 E_{xc}[\rho(\mathbf{r}/\lambda)/\lambda^3]\right). \tag{64}$$

For the homogeneous electron gas, $\epsilon_{xc,\lambda} = E_{xc,\lambda}/N$ is known accurately as a function of the electron density. Although $\epsilon_{xc,\lambda}$ for the uniform gas is not an analytic function of λ (due to the presence of terms like $\lambda \ln \lambda$), its coupling-constant dependence is otherwise similar to that of a finite system. In Figures 11 and 12 the coupling-constant dependence of $\epsilon_{xc,\lambda} = E_{xc,\lambda}/N$ for the homogeneous electron gas, as parametrized by Perdew and Wang[5], is shown. We consider two electron densities characterized by the Seitz radius $r_s = (3/4\pi\rho)^{1/3}$. The first, $r_s = 0.25$, is a typical density of core electrons in an atom or molecule. For high densities, the kinetic energy dominates the exchange-correlation energy. In finite systems such as atoms or molecules, we expect that $E_{xc,\lambda}[\rho]$ becomes

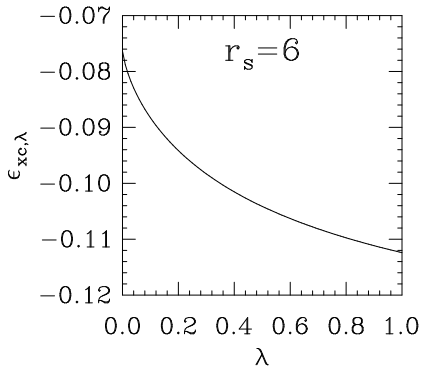

Figure 12. Same as Fig. 11, but at a low density, $r_s = 6$ *bohr*, typical of valence electrons.

linear in λ when the electron-electron interaction can be treated as a small perturbation, i.e., in the high-density limit. The correlation energy E_c can then be accounted for by second-order perturbation theory [53]. The curve in Fig. 11 is nearly linear, so the behavior of the homogeneous electron gas at high density is similar to that of a high-density finite system. For low densities, correlation effects become more important both in the homogeneous electron gas and in finite systems. In finite systems we then need higher-order perturbation theory to account for the correlation energy; second-order perturbation theory by itself overestimates the correlation energy, which saturates as $\lambda \to \infty$. Fig. 12 shows $\epsilon_{xc,\lambda}$ for a homogeneous electron gas with $r_s = 6$, which is typical of valence electrons in a low-density metal. The curve is strongly bent upward, a behavior expected also for a finite system of low density.

4.1. Coupling-constant averaged exchange-correlation energies

In the preceding section, we saw how to describe a physical system in terms of a fictitious non-interacting system and a correction term E_{xc} which accounts for the exchange-correlation energy of the electrons. The crucial point in this formulation of the many-electron problem is the approximation to be employed for E_{xc}. In Section 2 we saw how the PW91 approximation to E_x is constructed, so it remains to describe the approximation to $E_c = E_{xc} - E_x$. A detailed analysis of the PW91 construction of the correlation hole $\rho_c(\mathbf{r}, \mathbf{r}+\mathbf{u}) = \rho_{xc}(\mathbf{r}, \mathbf{r}+\mathbf{u}) - \rho_x(\mathbf{r}, \mathbf{r}+\mathbf{u})$ will be given in a forthcoming publication [42], so here we only state the main steps of this construction. As in the construction of the exchange hole, the correlation hole of the homogeneous electron gas of spin densities $\rho_\uparrow(\mathbf{r})$ and $\rho_\downarrow(\mathbf{r})$ defines the zeroth-order approximation to the correlation hole at $\mathbf{r}$ of

an inhomogeneous system with spin densities $\rho_\uparrow(\mathbf{r})$ and $\rho_\downarrow(\mathbf{r})$. The correlation hole of the homogeneous electron gas is not exactly known, but an accurate parametrization has been constructed [54]. To this hole a gradient correction is added. The resulting GEA correlation hole violates the normalization condition

$$\int d^3u \; \rho_c(\mathbf{r}, \mathbf{r}+\mathbf{u}) = 0 \tag{65}$$

on the correlation hole. This deficiency is rectified by a cutoff procedure completely analogous to the cutoff procedure which restores the normalization condition on the GEA expansion of the exchange hole. (Note however that the correlation hole does not have the constraint to be negative everywhere.) The numerical correlation energy functional defined by this procedure is then parametrized [17,19]. Again, the LSD on-top exchange correlation hole, while not exact [48], is highly accurate, and so helps explain the reliability of LSD exchange-correlation energies [49].

Table 3
Atomization energies (D_e) in the LSD and PW91 approximation. Unrestricted Hartree-Fock (UHF) and hybrid (as explained in section 5) results are also shown. LSD and PW91 energies are evaluated on LSD densities. The mean absolute errors (m.a.e.) are given separately for the singly- and multiply-bonded systems.

System	ΔE^{exact}	ΔE^{UHF}	ΔE^{LSD}	ΔE^{PW91}	ΔE^{hybrid}
H_2	.174	.136	.180	.168	.167
CH_4	.668	.523	.736	.672	.668
H_2O	.370	.248	.424	.376	.363
HF	.224	.154	.258	.228	.220
m.a.e.	-	.095	.040	.005	.005
CO	.413	.277	.476	.429	.406
N_2	.364	.183	.426	.386	.359
NO	.244	.084	.316	.273	.242
O_2	.192	.052	.279	.229	.198
m.a.e.	-	.154	.071	.026	.005

Local and semi-local approximations to $E_{xc,\lambda}$ are expected to work better at the upper end of the coupling-constant integration than at the lower end. Table 3 shows a remarkable improvement in the density functional approximations to E_{xc} over the approximations to E_x. As can be seen from Table 3, atomization energies are noticeably better in the PW91 approximation than in the LSD approximation. In general, we find that overestimation of the atomization energies at the exchange level carries over to the coupling-constant averaged quantities (but to a less severe extent), so that atomization energies of multiply-bonded systems are less accurately reproduced than atomization energies of singly-bonded systems.

With the coupling-constant integration in mind, we now propose an explanation of the results for the atomization energies. The atomization of a singly-bonded system will be

interpreted as a process involving an effective two-electron system with paired spins. The two-electron system is ideally realized in the H_2 molecule, and approximately in systems such as CH_4 where the binding electron pairs are separated from each other. For these systems we observe a smaller PW91 error at the exchange level than in the multiply-bonded systems, where the binding electron pairs interact strongly. In an effective two-electron process, the change in the exchange energy reduces to a change in the self-interaction energy, which seems to be well reproduced by the PW91 functional for exchange. In cases where two or more bonds are close to each other, we no longer have an effective two-electron system because there are several electrons with the same spin orientation in the same region of space. The LSD and to a lesser extent the PW91 approximation significantly overestimate the magnitude of the exchange energy in these cases, and this in turn leads to an overestimation of the coupling-constant averaged atomization energies. Presumably the density functionals overestimate the magnitude of the interelectronic exchange [26] here because they do not account for subtle effects of orbital nodality [55]. These functionals may also overestimate the magnitude of the self-exchange energy for the delocalized π orbitals.

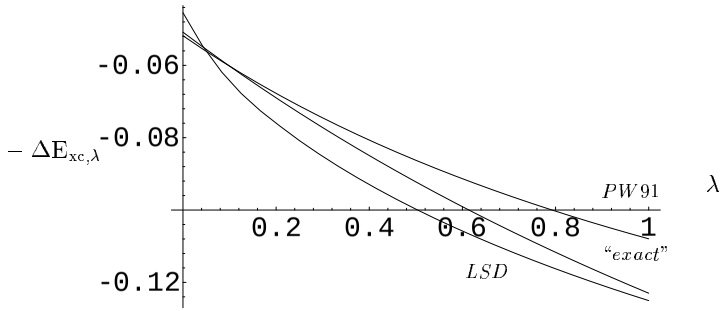

Figure 13. Sketch of $\Delta E_{xc,\lambda}$ for $H_2 \rightarrow 2H$. (Energy in hartrees.)

To understand the correlation contribution to the atomization energy, we consider the H_2 molecule where we have two anti-parallel-spin electrons in the molecular bond. To a limited extent the H_2 molecule already shows static or 'left-right' correlation, which becomes more pronounced if we stretch the bond length, and less pronounced if we shorten it. Static correlation causes a more rapid drop of $-\Delta E_{xc,\lambda}$ for small λ, followed by a flattening of the curve, i.e., a stronger concavity. Local and semi-local approximations do not accurately account for this static correlation, but are more appropriate for the description of dynamic correlation. In the presence of static correlation, since $-\Delta E_{c,\lambda}$

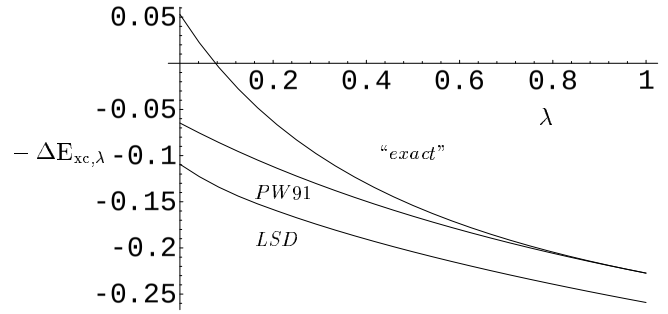

Figure 14. Sketch of $\Delta E_{xc,\lambda}$ for $N_2 \rightarrow 2N$. (Energy in hartrees.)

for the approximate functionals is less concave as a function of λ than the exact curve, such functionals are likely to underestimate the magnitude of the correlation energy in the molecule: The exact slope of $-\Delta E_{xc,\lambda}$ at $\lambda = 0$ is more negative than the approximate one. In cases where the exchange contribution to the atomization energy is accurately reproduced (as in H_2 at the equilibrium bond length), the total atomization energy is then underestimated.

For multiply-bonded systems like N_2, the LSD and PW91 overestimation of the ΔE_x contribution to the atomization energy is only partly compensated by underestimation of ΔE_c. Cases intermediate between the H_2 molecule and the N_2 molecule are for instance CH_4 and H_2O, where the described errors in the differential exchange-correlation effects approximately cancel, i.e., the overestimation of ΔE_x is compensated by an underestimation of ΔE_c.

To illustrate these arguments, we sketch the coupling-constant dependence of $\Delta E_{xc,\lambda}$ for H_2 and N_2. $\Delta E^{LSD}_{xc,\lambda}$ and $\Delta E^{PW91}_{xc,\lambda}$ in Figs. 13 and 14 are calculated using Eq. 64, while the "exact" curve for H_2 is a sketch which reproduces the correct exchange limit, the experimental value for ΔE_{xc} and the correct value for $\Delta E_{xc,\lambda=1}$ [56]. The "exact" curve for N_2 is an interpolation between the exact $\Delta E_{xc,\lambda=0}$ and $\Delta E^{PW91}_{xc,\lambda=1}$, which yields the experimental ΔE_{xc}.

For the H_2 molecule the PW91 approximation gives good results for ΔE_x. Due to the missing weak static correlation, $-\Delta E_{xc,\lambda=1}$ is insufficiently negative in the PW91 approximation, so that ΔE_{xc} is slightly underestimated. The LSD approximation overestimates the dynamic correlation contribution to ΔE_{xc}.

The N_2 molecule shows much stronger static correlation (expected to be most pronounced within each π bond) which is mimicked by the large PW91 exchange energy error, so that $\Delta E^{PW91}_{xc,\lambda=1}$ is very accurate. Because the PW91 curve in Fig. 14 is too flat, it predicts an atomization energy for the N_2 molecule which is too large. Strong static

correlation in the molecule causes the exact $-\Delta E_{xc,\lambda}$ to drop rapidly from its $\lambda = 0$ value towards its $\lambda = 1$ value. The separated atoms do not have much static correlation, so $E_{xc,\lambda}$ can be accurately obtained from second-order perturbation theory, which implies that $E_{xc,\lambda}^{atoms}$ is close to a straight line. The LSD curve overestimates $\Delta E_{xc,\lambda}$ at $\lambda = 1$, but its error is smaller there than at the $\lambda = 0$ end.

5. Hybrids of Hartree-Fock with density functional theory

The Hartree-Fock approximation is exact in the very limit ($\lambda = 0$ or exchange-only) where local or semi-local density functionals are often least accurate. This realization led Becke to propose the approximation [14,23]

$$E_{xc}^{hybrid} = E_{xc}^{GGA} + a_0(E_x - E_x^{GGA}), \tag{66}$$

where E_x is the exact exchange energy (the Fock integral of Eq. 7, evaluated with LSD or GGA orbitals), and $a_o \approx 0.28$ is an empirical parameter. The "hybrid" of Eq.66 is also known as the "adiabatic connection" or "exact exchange mixing" formula.

Eq. 66 is a way to refine the coupling constant integral of Eq. 60 through replacement of GGA by exact information about the lower limit $\lambda = 0$, as in our construction of the "exact" curve of Fig. 14. We have recently argued [28] that this construction leads to $a_0 \approx 1/n$, where n is the lowest order of density functional perturbation theory that yields accurate atomization energies, whence $n = 4$ for typical molecules described by a fourth-order Møller-Plesset (MP4)-like expansion. At this level, $\Delta E_{xc,\lambda}$ is a cubic in λ. Table 3 shows that this nonempirical $n = 4$ hybrid brings the PW91 atomization energies close to the goal of chemical accuracy.

Hybrids more sophisticated than Eq. 66 can be constructed by using additional information about $\Delta E_{xc,\lambda}$, such as the GGA value at $\lambda = 1$ [27] or the exact derivative $d\Delta E_{xc,\lambda}/d\lambda$ at $\lambda = 0$ from second-order density functional perturbation theory [28,57]. Although further improvements in accuracy may result, this accuracy is ultimately limited by the residual GGA errors that persist far from the $\lambda \to 0$ limit.

6. Conclusions

Both exchange and correlation contribute heavily to the atomization energy of a molecule. While exchange is treated exactly in Hartree-Fock theory, even a simple local-spin density (LSD) approximation to exchange and correlation does better than Hartree-Fock alone. Further improvements in atomization energies are achieved by adding gradient corrections (GGA's or semi-local approximations), and by hybridizing 25% (but not 100 %!) of the exact exchange energy with GGA.

Local and semi-local density functionals work, not only because they are exact for a uniform or slowly-varying density, but more directly because they respect exact constraints on the exchange-correlation hole (Eqs. 27,29,65). For LSD and for the PW91 GGA, we have extracted the model exchange holes for comparison with the exact one (Figs. 9 and 10). After (but only after) system- and spherical averaging, we find that these holes are realistic. The inhomogeneity or gradient corrections to LSD correctly produce a hole which is deeper close to the electron and shallower far away, and thus an exchange energy that is more negative than that of LSD.

The exchange-correlation energy is a coupling-constant integral (Eq. 60), and local or semi-local approximations typically work better at the fully-interacting or $\lambda = 1$ end, where the hole is deepest and most short-ranged, than at the $\lambda = 0$ (exchange) end. GGA exchange is more accurate than LSD exchange, but the pattern of error is different: While LSD is more accurate for the molecule than for the separated atoms, GGA is more accurate for the atoms. Moreover, we can distinguish between singly-bonded molecules, for which GGA exchange is quite accurate, and multiply-bonded molecules, for which GGA makes the exchange energy too negative. We interpret this to mean that GGA describes "self-exchange" accurately (at least for the σ bonds) but exaggerates the "interelectronic exchange" between parallel-spin electrons in neighboring bonds.

On the other hand, the GGA for the correlation energy misses some of the static or "left-right" correlation between two anti-parallel spin electrons in a bond, and so does not make the correlation energy of the molecule negative enough. The two GGA errors (in exchange and in correlation) tend to cancel, but the cancellation is not uniform over all molecules. In H_2, the exchange error is negligible while the correlation error is not, so GGA underestimates the atomization energy. In N_2, the exchange error is dominant, so GGA overestimates the atomization energy. In CH_4, the two errors very neatly cancel.

Because the exchange errors of GGA tend to be the most severe ones, quite accurate atomization energies can be found by mixing a fraction of the exact exchange energy with GGA. Moreover, this fraction can be estimated non-empirically.

Acknowledgments

This work was supported in part by the Deutsche Forschungsgemeinschaft, and in part by the National Science Foundation under Grant DMR95-21353.

Appendix: Technical details of the calculations

The Kohn-Sham calculations are performed with a modified version of the CADPAC program [41]. The electron densities are obtained from unrestricted Kohn-Sham calculations in the LSD approximation, and the various functionals have been evaluated on these densities. Nonspherical densities and Kohn-Sham potentials have been used for open-shell atoms [60]. The experimental geometries employed in our work are listed in Refs. [61]. The D_e values are obtained from the experimental atomization energies and the zero point energies given in Refs. [62]. The gaussian basis sets used are of triple zeta quality with p- and d- type polarization functions for the hydrogen and d- and f-type polarization functions for the second-row elements.

The results for the exchange holes are based on Hartree-Fock calculations performed with the COLUMBUS program system [58,59]. Gaussian basis sets close to the Hartree-Fock limit are used, and the resulting two-particle density matrix in the basis set representation is transformed to the real-space representaion of the exchange hole.

REFERENCES

1. R. G. Parr and W. Yang, *Density-Functional Theory of Atoms and Molecules* (Oxford University Press, Oxford, 1989).

2. R. M. Dreizler and E. K. U. Gross, *Density Functional Theory* (Springer Verlag, Berlin, 1990).
3. W. Kohn and L. J. Sham, Phys. Rev. **140**, A1133 (1965).
4. A. Szabo and N. S. Ostlund, *Modern Quantum Chemistry* (Macmillan Publishing, New York, 1982).
5. J. P. Perdew and Y. Wang, Phys. Rev. B **45**, 13244 (1992).
6. S.-K. Ma and K. A. Brueckner, Phys. Rev. **165**, 18 (1968).
7. L. J. Sham, in *Computational Methods in Band Theory*, edited by P. Marcus, J. F. Janak, and A. R. Williams (Plenum, New York, 1971).
8. O. Gunnarsson and B. I. Lundqvist, Phys. Rev. B **13**, 4274 (1976).
9. D. C. Langreth and J. P. Perdew, Phys. Rev. B **21**, 5469 (1980).
10. D. C. Langreth and M. J. Mehl, Phys. Rev. B **28**, 1809 (1983).
11. A. D. Becke, J. Chem. Phys. **84**, 4524 (1986).
12. A. D. Becke, Phys. Rev. A **38**, 3098 (1988).
13. C. Lee, W. Yang, and R. G. Parr, Phys. Rev. B **37**, 785 (1988).
14. A. D. Becke, J. Chem. Phys. **104**, 1040 (1996).
15. J. P. Perdew, Phys. Rev. B **33**, 8822 (1986).
16. J. P. Perdew and Y. Wang, Phys. Rev. B **33**, 8800 (1986).
17. J. P. Perdew, in *Electronic Structure of Solids 91*, edited by P. Ziesche and H. Eschrig (Akademie Verlag, Berlin, 1991).
18. J. P. Perdew, J. A. Chevary, S. H. Vosko, K. A. Jackson, M. R. Pederson, D.J. Singh, and C. Fiolhais, Phys. Rev. B **46**, 6671 (1992); **48**, 4978 (1993) (E).
19. J. P. Perdew, K. Burke, and Y. Wang, submitted to Physical Review B.
20. A. D. Becke, J. Chem. Phys. **97**, 9173 (1992).
21. B. G. Johnson, P. M. W. Gill, and J. A. Pople, J. Chem. Phys. **98**, 5612 (1993).
22. J. M. Seminario, Chem. Phys. Lett. **206**, 547 (1993).
23. A. D. Becke, J. Chem. Phys. **98**, 1372 (1993).
24. A. D. Becke, J. Chem. Phys. **98**, 5648 (1993).
25. A. Görling and M. Levy, unpublished.
26. M. Ernzerhof, K. Burke, and J. P. Perdew, submitted to the International Journal of Quantum Chemistry Symposium.
27. K. Burke, M. Ernzerhof, and J. P. Perdew, submitted to Chemical Physics Letters.
28. J. P. Perdew, K. Burke, and M. Ernzerhof, submitted to the Journal of Chemical Physics.
29. *Ab Initio Methods in Quantum Chemistry I and II*, *Advances in Physical Chemistry*, edited by K. Lawley (Wiley, New York, 1987).
30. G. L. Oliver and J. P. Perdew, Phys. Rev. A **20**, 397 (1979).
31. M. Levy and J. P. Perdew, Phys. Rev. A **32**, 2010 (1985).
32. M. Levy, Phys. Rev. A **43**, 4637 (1991).
33. J. D. Talman and W. F. Shadwick, Phys. Rev. A **14**, 36 (1976).
34. V. Sahni, J. Gruenebaum, and J. P. Perdew, Phys. Rev. B **26**, 4371 (1982).
35. M. K. Harbola and V. Sahni, Phys. Rev. Lett. **62**, 489 (1989).
36. J. B. Krieger, Y. Li, and G. J. Iafrate, Phys. Rev. A **45**, 101 (1992).
37. A. Görling and M. Ernzerhof, Phys. Rev. A **51**, 4501 (1995).
38. M. A. Buijse and E. J. Baerends, in *Density Functional Theory of Molecules, Clusters,*

and Solids, edited by D. E. Ellis (Kluwer Academic, Dordrecht, 1995).
39. M. Ernzerhof, J. P. Perdew, and K. Burke, in *Density Functional Theory*, edited by R. Nalewajski (Springer-Verlag, Berlin, 1996), to appear.
40. T. Ziegler, A. Rauk, and E. J. Baerends, Theoret. Chim. Acta **43**, 261 (1977).
41. CADPAC6: The Cambridge Analytical Derivatives Package Issue 6.0 Cambridge (1995) A suite for quantum chemistry programs developed by, R. D. Amos, with contributions from I.L. Alberts, J.S. Andrews, S.M. Cowell, N.C. Handy, D. Jayatilaka, P.J. Knowles, R. Kobayashi, N. Noga, K.E. Laidig, P.E. Maslan, C.W. Murray, J.E. Rice, J. Sanz, E.D. Simandrias, A.J. Stone, M.-D. Su, and D.J. Tozer.
42. K. Burke, M. Ernzerhof, and J. P. Perdew, in preparation.
43. Y. Wang, J. P. Perdew, J. A. Chevary, L. D. MacDonald, and S. H. Vosko, Phys. Rev. A **41**, 78 (1990).
44. L. Kleinman and S. Lee, Phys. Rev. B **37**, 4634 (1988).
45. M. Slamet and V. Sahni, Phys. Rev. B **44**, 10921 (1991).
46. J. P. Perdew, K. Burke, and M. Ernzerhof, submitted to Physical Review Letters.
47. J. P. Perdew and K. Burke, Int. J. Quantum Chem. Symposium **57**, 309 (1996).
48. K. Burke, J. P. Perdew, and D. C. Langreth, Phys. Rev. Lett. **73**, 1283 (1994).
49. K. Burke, J. P. Perdew, and M. Ernzerhof, in preparation.
50. D. C. Langreth and J. P. Perdew, Solid State Comm. **17**, 1425 (1975).
51. D. C. Langreth and J. P. Perdew, Phys. Rev. B **15**, 2884 (1977).
52. M. Levy, N.H. March, and N.C. Handy, J. Chem. Phys. **104**, 1989 (1996).
53. A. Görling and M. Levy, Phys. Rev. A **50**, 196 (1994).
54. J. P. Perdew and Y. Wang, Phys. Rev. B **46**, 12947 (1992).
55. O. Gunnarsson and R. O. Jones, Phys. Rev. B **31**, 7588 (1985).
56. O. Gritsenko, R. van Leeuwen, and E. J. Baerends, preprint.
57. M. Ernzerhof, J. P. Perdew, and K. Burke, in preparation.
58. R. Shepard, I. Shavitt, R. M. Pitzer, D. C. Comeau, M. Pepper, H. Lischkau, P. G. Szalay, R. Ahlrichs, F. B. Brown, and J.-G. Zhoa, Int. J. Quantum Chem. **142**, 22 (1988).
59. R. Shepard, H. Lischka, P. G. Szalay, T. Kovar, and M. Ernzerhof, J. Chem. Phys. **96**, 2085 (1992).
60. F.W. Kutzler and G.S. Painter, Phys. Rev. Lett. **59**, 1285 (1987).
61. D.J. DeFrees, B.A. Levi, S.K. Pollack, W.J. Hehre, J.S. Binkley, and J.A. Pople, J. Am. Chem. Soc. **101**, 4085 (1979). Geometry of *NO*: K.P. Huber and G. Herzberg, *Molecular Spectra and Molecular Structure IV: Constants of Diatomic Molecules*, Van Nostrand Reinhold, New York, 1979.
62. J.A. Pople, M. Head-Gordon, D.J. Fox, K. Raghavachari, L.A. Curtiss, J. Chem. Phys. **90**, 5622 (1989); L.A. Curtiss, C. Jones, G.W. Trucks, K. Raghavachari, and J.A. Pople, J. Chem. Phys. **93**, 2537 (1990).